

A high-order discrete scheme of Lattice Boltzmann method for cavitation simulation

¹Min Zhong, ²Chengwen Zhong, ³Cunru Bai

¹ National Key Laboratory of Science and Technology on Aerodynamics Design and Research, Northwestern Polytechnical University, Xi'an, China

^{*2} National Key Laboratory of Science and Technology on Aerodynamics Design and Research, Northwestern Polytechnical University, Xi'an, China

³ National Key Laboratory of Science and Technology on Aerodynamics Design and Research, Northwestern Polytechnical University, Xi'an, China

Email: zhongcw@nwpu.edu.cn

Abstract –The cavitation is defined as the process of formation of the vapor of liquid when it is subjected to reduced pressure at constant ambient temperature, including the process of formation, developing and breaking. Cavitation is a significant cause of wear in some engineering contexts and plays a destruction role in the aspect of fluid machinery, but supercavitation can be used to envelope an underwater device or vessel and allow it to travel at greatly increased speed by significant reduction of the drag. In present paper, high order isotropic discrete scheme and the Carnahan-Starling real-gas equation of state (C-S EOS) are coupled in the Shan-Chen multiphase lattice Boltzmann model. The reduction of the spurious current is simulated in the condition of the high order isotropic discrete scheme of force term, and the complete cavitation process of a bubble is also reproduced successfully. The relationships between the radius of bubble seed and cavitation for a density ratio of 50-200 have been investigated by Lattice Boltzmann method with the high-order isotropic discrete scheme.

Keywords –Two phase flow; Lattice Boltzmann method; Isotropic; Cavitation

1. Introduction

The cavitation is the sudden onset of vapor bubbles in a flow due to the pressure falling below the liquid's vapor pressure [1], which plays a destruction role in the aspect of fluid machinery, propeller in the propulsion device, or the cascades of turbomachinery. But supercavitation can be used to envelope an underwater vehicle by significant reduction of the drag. So it has important significance for the research of cavitation inception.

The occurrence of cavitation is not only due to the vapor pressure of the fluid, but also has a direct relationship with the size and the number of cavitation bubble nuclei in the liquids. In the past few decades, numerous efforts have contributed to the study of cavitation inception. Lauterborn et al. [2] studied the dynamics of cavitation bubbles which are produced with laser. Blake et al [3] experimentally analyzed the dynamics of cavitation bubble collapse and its influence on boundaries and the flow domain. Or and Tuller [4] discussed the relationship between the radius of nuclei and the cavitation. All these efforts can contribute to the research of cavitation in the future.

The lattice Boltzmann methods (LBM) has emerged as a new numerical method in the late 80s of last century. In the LBM [5], the fluid has been abstracted for the large number of fictive particles, and such particles perform consecutive stream and collision processes over a discrete lattice mesh. Through the statistics of the distribution function of these particles, we can get the macroscopic features of fluid motion. In recent twenty years, LBM has been applied in many areas, especially in multiphase flow [6-8]. Its application to multiphase flow first started in

1991 when Gunstensen [9] proposed the color-model, which based on lattice gas automata model. Grunau et al [10] popularized this model to the multiphase flow system in which the density and viscosity is changeable. In 1993, Shan and Chen [11] advanced a pseudo-potential model, which has been widely used. In 1996, Swift et al [12] proposed a free energy model which allowed adjusting the width of the gas-liquid interface. Lee and Lin [13] applied different discrete format before and after the collision based on the free energy model.

In our daily life, Liquid is very common, such as water and air. The density ratio between the liquid and the gas is generally great up to 10^3 or higher. So the large density ratio models attract great attention. Peng et al [14] compared different EOSs applied in Shan-Chen model. Excellent performance of C-S EOS is employed in multiphase flow simulations with the density ratio over 10^3 . Lee-Lin [13] simulated droplet with the density ratio of 10^3 . Rising of single bubble with the density ratio of 10^3 is simulated by Inamuro et al [15]. But 2D bubble evolution was subjected to certain restrictions of density ratio in the numerical simulation. Sukop [16] simulated two-dimensional cavitation based on Shan-Chen model with a low density ratio. Zhang et al [17] simulated three-dimensional cavitation with density ratio close to 10, and Chen et al [18] improved the density ratio to 200. In all these LBM simulations for 2D bubble evolution, some of these enhance the density ratio, but do not analyze the spurious currents which will lead to instability of numerical simulation process.

In this paper, Shan-Chen model combined with the high order discrete scheme for force term in LBM is constructed in cavitation simulation. The high order

discrete format is helpful to reduce the spurious currents, and C-S EOS is available to enlarge the density ratio. Reduction of spurious current with higher-order isotropic tensors is analyzed in our work. In addition, the relationship between the radius of nuclei and cavitation is also analyzed. We succeeded to simulate bubble growth or collapse with the density ratio of 70-200 in the conditions of higher-order discrete scheme.

2. Mathematical models and the computational domain

2.1. Mathematical model

The typical LB equation with external force term is presented as

$$f_i(\mathbf{x} + \mathbf{e}_i \Delta t, t + \Delta t) = f_i(\mathbf{x}, t) - \frac{1}{\tau} [f_i(\mathbf{x}, t) - f_i^{eq}(\mathbf{x}, t)] + \Delta f_i, \quad (1)$$

where $f_i(\mathbf{x}, t)$ denotes the particle velocity distribution function along the i th direction at time t and position \mathbf{x} , $f_i^{eq}(\mathbf{x}, t)$ corresponding local equilibrium distribution, \mathbf{e}_i is the particle velocities along the i th direction. τ is the collision relaxation time, Δf_i is the body force term, Δt is time interval, $\Delta t \equiv 1$. In this paper, D2Q9 model is applied. The equilibrium distribution reads

$$f_i^{eq}(\mathbf{x}, t) = \omega_i \rho(\mathbf{x}) \left[1 + 3 \frac{\mathbf{e}_i \cdot \mathbf{u}}{c^2} + \frac{9}{2} \frac{(\mathbf{e}_i \cdot \mathbf{u})^2}{c^4} - \frac{3}{2} \frac{\mathbf{u}^2}{c^2} \right], \quad (2)$$

where ω_i is the weights, ω_i is $4/9$ ($i=0$), $1/9$ ($i=1,2,3,4$), $1/36$ ($i=5,6,7,8$), c is the speed of the lattice, $c \equiv 1$. \mathbf{u} is the macroscopic speed, ρ is the macroscopic density. The corresponding macroscopic variables are defined as

$$\rho = \sum_i f_i, \quad (3)$$

$$\mathbf{u} = \frac{1}{\rho} \sum_i f_i \cdot \mathbf{e}_i, \quad (4)$$

$$\tau = \frac{1}{2} + 3\nu, \quad (5)$$

where ν is kinematic viscosity.

According to Shan-Chen model, the interaction force F between particles is expressed as

$$F = -G\psi(\mathbf{x}) \sum_i w(|\mathbf{e}_i|^2) \psi(\mathbf{x} + \mathbf{e}_i) \mathbf{e}_i, \quad (6)$$

where G is interaction strength, $G=-7$.

According to Ref. [19], the interaction force F can be determined by the requirement that the finite difference gradient operator should possess sufficient degree of isotropy so as to reduce the extent of the spurious current in the vicinity of a curved interface.

Following the analysis of finite difference schemes. applying the Taylor expansion, Eq.(6) can be expressed as

$$F = -G\psi(\mathbf{x}) \left(E_{ij}^{(2)} \partial_j \psi + \frac{1}{3!} E_{ijkl}^{(4)} \partial_{jkl} \psi + \frac{1}{5!} E_{ijklpq}^{(6)} \partial_{jklpq} \psi + \frac{1}{7!} E_{ijklpqst}^{(8)} \partial_{jklpqst} \psi + \dots \right), \quad (7)$$

where $E^{(m)} = E_{i_1 i_2 \dots i_m}^{(m)} = \sum_{\alpha} w(|\mathbf{e}_{\alpha}|^2) e_{\alpha}^{i_1} e_{\alpha}^{i_2} \dots e_{\alpha}^{i_m}$. In this paper,

we only discuss the highest order up to 10. The weight coefficients in Eq.(7) are selected according to Table 1.

The simplified pressure is obtained based on Shan-Chen model

$$P = \frac{\rho}{3} + \frac{G}{6} (\psi(\rho))^2, \quad (7)$$

Instead of giving ψ directly, it can be calculated from EOS, namely.

$$\psi(\rho) = \sqrt{\frac{6(p - \rho c_s^2)}{g}}, \quad (8)$$

In Eq.(9), p is determined by the Carnahan-Starling equation of state:

$$p = \rho RT \frac{1 + b\rho/4 + (b\rho/4)^2 - (b\rho/4)^3}{(1 - b\rho/4)^3} - a\rho^2, \quad (9)$$

where $a = 0.4963R^2 T_c^2 / P_c$, $b = 0.1827RT_c / P_c$, $a=1$, $b=4$, $R=1$.

In the Eq.(1) the external force is expressed as

$$\Delta f_i = f_i^{eq}(\rho, \mathbf{u} + \Delta \mathbf{u}) - f_i^{eq}(\rho, \mathbf{u}), \quad (11)$$

where $\Delta \mathbf{u} = \mathbf{F} \Delta t / \rho$.

Table 1. Weight coefficients that yield isotropic $E^{(n)}$ tensors

| | W(1) | W(2) | W(4) | W(5) | W(8) | W(9) | W(10) |
|------------|----------|---------|-------|-------|--------|--------|--------|
| $E^{(4)}$ | 1/3 | 1/12 | | | | | |
| $E^{(6)}$ | 4/15 | 1/10 | 1/120 | | | | |
| $E^{(8)}$ | 4/21 | 4/45 | 1/60 | 2/315 | 1/5040 | | |
| $E^{(10)}$ | 262/1785 | 93/1190 | 7/340 | 6/595 | 9/9520 | 2/5355 | 1/7140 |

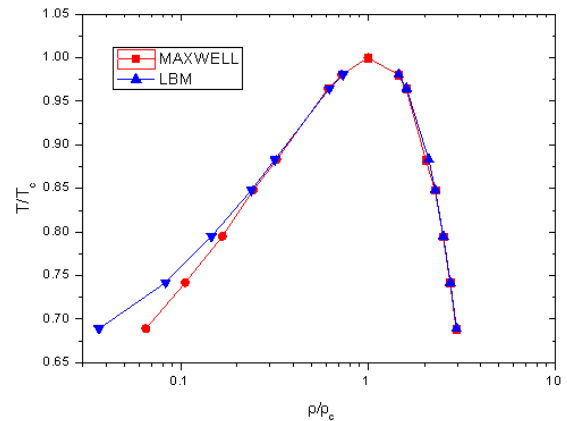


Figure 1. Coexistence curves (LBM and MAXWELL)

In order to check the feasibility of the high order discrete scheme, we compare the value of density based on 10 order discrete format with Maxwell equal-area rule. In Fig.1, we can see that high order discretization scheme is a good match with Maxwell equal-area rule, especially for the liquid density. However, the vapor density will result in a deviation with the density ratio increasing.

2.2. The computational domain

To compare the spurious currents based on high order discretization, a computational domain of 100×100 with periodic boundary conditions is adopted. The density ratio of 60-200 is captured successfully. In addition, the computational domain, 201×201 , is set for simulating cavitation. The constant pressure boundary conditions is imposed on the left and right boundaries, and the periodic boundary conditions is applied on upper and lower boundaries, which will promote fluid flow and create an environment for the occurrence of cavitation. In this paper, 10-order isotropic discrete scheme is adopted for simulating cavitation with the density of 70 and 200. The interfacial tension, $\sigma = \Delta P \cdot r$, is obtained for bubbles or droplets. The nuclei (with the corresponding initial density ratios 70, 200 roughly) are chosen for discussing about bubble growth or collapse.

Results and discussion

3.1. Spurious currents

Shan [20] has proposed that high-order isotropic discrete play an important role in the reduction of spurious current. Sbragalia [19] support these previous findings and push isotropy to higher, and show the change of spurious currents with a density ratio of 60. To reproduce Sbragalia's numerical results, we fix the pseudo potential shape to $\psi = 1 - \exp(-\rho)$ [19] and report spurious currents around a static drop of radius 20 and density ratio $\Delta\rho / \rho_v \sim 60$. In Fig. 2, the different plots correspond to different degrees of isotropy (4-order, 6-order, 8-order, 10-order separately). Numerical results (see Fig.2) do confirm a decay of the magnitude of the spurious contributions with the raise of the order of isotropy. In this paper, to enlarge the density ratio, the C-S EOS is coupled in the Shan-Chen multiphase lattice Boltzmann model. In Fig.3, the spurious contributions for a static drop are analyzed for a density ratio $\Delta\rho / \rho_v \sim 60$. Comparing with Fig.2, the pseudo-speed in Fig.3 will be lower nearly an order of magnitude. Fig.4 shows a reduction of spurious currents with a density ratio of 200. All these results show that the magnitude of the spurious currents is significantly reduced as the higher order isotropy is employed.

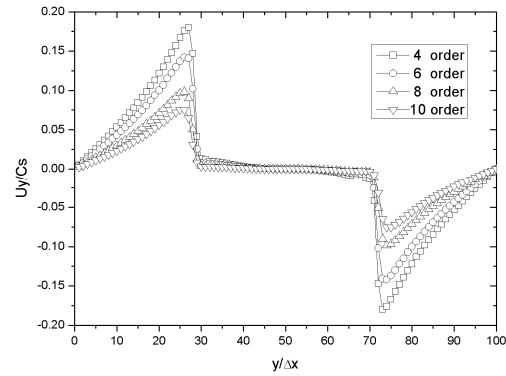


Figure 2. Reduction of spurious currents based on Sbragalia' pseudo-potential function ($\Delta\rho / \rho_v \sim 60$)

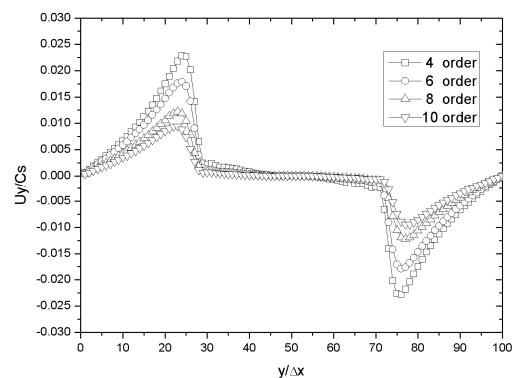


Figure 3. Reduction of spurious currents with higher order isotropic tensors base on C-S EOS ($\Delta\rho / \rho_v \sim 60$)

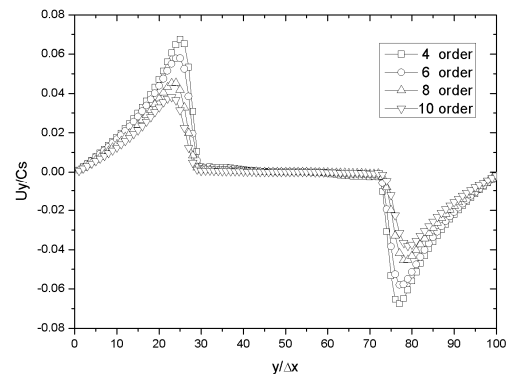


Figure 4. Reduction of spurious currents with higher order isotropic tensors base on C-S EOS($\Delta\rho / \rho_v \sim 200$)

3.2. Cavitation simulation based on high-order discrete scheme

According to the analysis of the spurious currents with high-order discrete scheme, it is bound to reduce the spurious currents of the whole cavitation process. Bubble growth or collapse is simulated with 10-order discrete scheme and the relationships between the radius of nuclei and cavitation is analyzed. Simulation results are consistent with the theoretical results, namely, a nucleus with a radius less than r^* will be lost to condensation and

a nucleus with a radius just above r^* acts as a seed for cavitation. Therefore, we achieved the simulation of cavitation in the conditions of low spurious currents.

Fig.5 and Fig.8 show the relationships between the radius of nuclei and cavitation. Two temperatures, $T=0.0655$, 0.0615 are tested. In the Fig.5 and Fig.6, $T=0.0655$ is chosen and the corresponding density ($\rho_v=0.00495377$, $\rho_l=0.362368$) is applied for bubble growth or collapse. The interfacial tension $\sigma=0.02002349$ and critical radius $r^*=10.7$ are applied. In the Fig.7 and Fig.8, $T=0.0615$ is set and the corresponding density ($\rho_v=0.00192797$, $\rho_l=0.383221$) is applied for bubble growth or collapsed. The interfacial tension $\sigma=0.026778$ and critical radius $r^*=9.72698$ are applied.

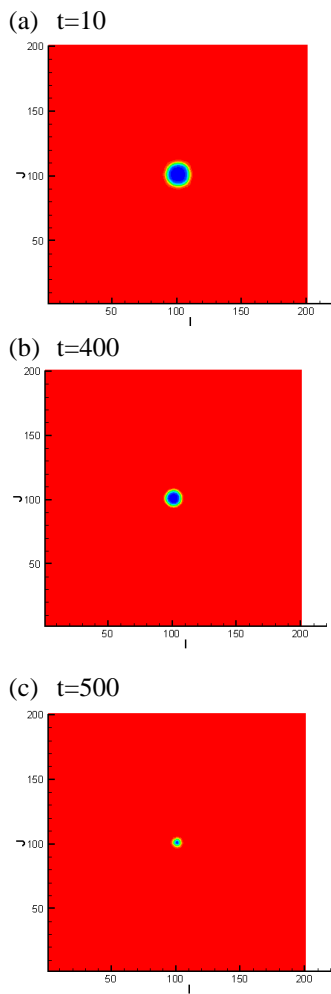


Figure 5. Vapour condensation on bubble collapse ($\Delta\rho/\rho_v \sim 70$, $r=9$)

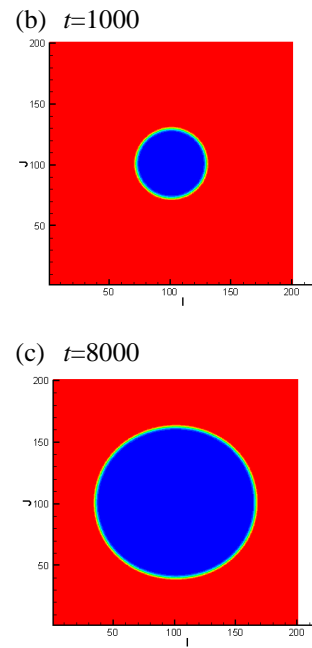
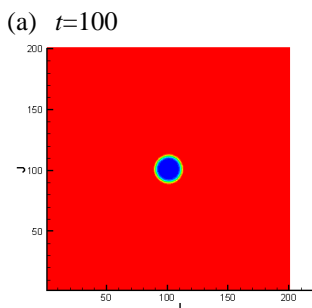


Figure 6. Growth of cavitation bubble nuclei ($\Delta\rho/\rho_v \sim 70$, $r=11$)

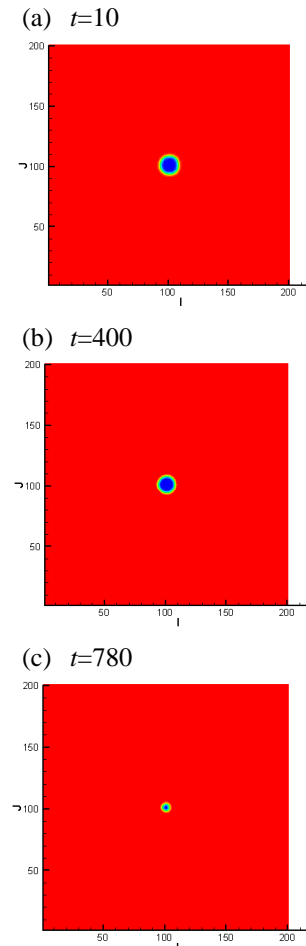


Figure 7. Vapour condensation on bubble collapse ($\Delta\rho/\rho_v \sim 200$, $r=8$)

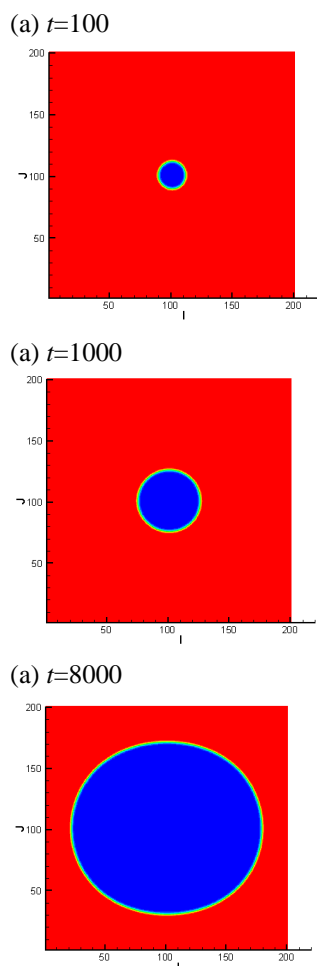


Figure 8. Growth of cavitation bubble nuclei ($\Delta\rho/\rho_v \sim 200$, $\tau=11$)

4. Conclusions

In this paper, a high-order isotropic discretization scheme of force term in LBM and C-S EOS are coupled in Shan-Chen model. The C-S equation of state is applied to obtain the large density ratio, and the high-order isotropic discrete scheme contributed to the spurious currents decreasing. We successfully simulated cavitation based on Shan-Chen model with high-order isotropic discretization scheme and C-S EOS and the numerical results is in accordance with the theoretical results [4]. We expect to apply the model to more complex problems where highly isotropic calculation of gradients is required.

References

- [1] Brennen C E, Cavitation and Bubble Dynamics, Oxford University Press, New York, 1995
- [2] Lauterborn W, Ohl C D, Cavitation bubble dynamics, Ultrason. Sonochem, 4(1997) 65
- [3] Blake J R, Gibson D C, Cavitation bubbles near boundaries, Ann. Rev. Fluid Mech. 19(1987) 99
- [4] Or D, Tuller M, Cavitation during desaturation of porous media under tension, Water Resour. Res. 38(2002) 1601
- [5] Qian Y H, D'huimères D, Lallemand P, Lattice BGK Models for Navier-Stokes Equation, Europhys. Lett. 17(1992) 479
- [6] Bower A L, Lee T, Single bubble rising dynamics for moderate Reynolds number using Lattice Boltzmann Method, Comput. Fluids, 39(2010) 1191
- [7] Zhong C W, Xie J F, Zhuo C S, Xiong S W, Yin D C, Simulation of natural convection under high magnetic field by means of the

thermal lattice Boltzmann method, Chinese Phys. B, 18(2009) 4083

- [8] Gupta A, Kumar R, Lattice Boltzmann simulation to study multiple bubble dynamics, Int. J. Heat and Mass Transfer, 51(2008) 5192
- [9] Gunstensen A K, Rothman D H, Zaleski S, Zanetti G, Lattice Boltzmann model of immiscible fluids, Phys. Rev. A, 43(1991) 4320
- [10] Grunau D, Chen S, Eggert K, A lattice Boltzmann model for multi-phase fluid flows, Phys. Fluids A, 5(1993) 2557
- [11] Shan X, Chen H, Lattice Boltzmann model for simulating flows with multiple phases and phases and components, Phys. Rev.E, 47(1993) 1815
- [12] Lee T, Lin C L, A stable discretization of the lattice Boltzmann equation for simulation of incompressible two-phase flows at high density ratio, J. Comput. Phys. 206(1993) 16
- [13] Swift M R, Orlandini E, Osborn W R, Yeomans J M, Lattice Boltzmann simulations of liquid-gas and binary fluid systems, Phys. Rev. E, 54(1996) 5041
- [14] Peng Y, Laura S, Equations of state in a lattice Boltzmann model, Phys. Fluids, 18(2006) 042101
- [15] Inamuro T, Ogata T, Ogino F, Numerical simulation of bubble flows by the lattice Boltzmann method, Gener. Comp. Sy. 20(2004) 959
- [16] Sukop M, Or D, Lattice Boltzmann method for homogeneous and heterogeneous cavitation, Phys. Rev. E, 71(2005) 046703
- [17] Zhang M, Zhou C Y, Shams I, Liu J Q, Three-dimensional cavitation simulation using lattice Boltzmann method, Acta Phys. Sin. 58(2009) 8406
- [18] Chen X P, Zhong C W, Yuan X L, Lattice Boltzmann simulation of cavitating bubble growth with large density ratio, Comput. Math. Appl. 12(2011) 3577
- [19] Sbragaglia M, Benzi R, Biferale L, Succi S, Sugiyama K, Toschi F, Generalized lattice Boltzmann method with multirange pseudopotential, Phys. Rev. E, 75(2007) 026702
- [20] Shan X W, Analysis and reduction of the spurious current in a class of multiphase lattice Boltzmann models, Phys. Rev. E, 73(2006) 04770
- [21] Arash Ahmadvand, Enhancement of L-junction Plasmon Waveguides Properties Using Various Shapes of Au Nanoparticles Arrays at $\lambda \approx 1550\text{nm}$, Advances in Digital Multimedia, 1(2011), 1-3
- [22] Zhang Y., Wu L., Rigid Image Registration by PSOSQP Algorithm, Advances in Digital Multimedia, 1(2011), 4-8
- [23] Amir Ghoreishi S., Application of Optimal Control Pole-placement and Fuzzy PID Controller in the New Model of the Macpherson Suspension System, Advances in Digital Multimedia, 1(2011), 9-18